4
Investigation of Resistive Switching from PVP:MoS_2/TiO_2 Hybrid Bilayer

In this chapter, the switching behavior of a bilayer comprising a PVP:MoS_2 and TiO_2 for use in RRAM devices on both rigid (glass) and flexible PEN substrates are investigated. Both devices demonstrated excellent switching performance with low SET and RESET voltages and high I_{ON}/I_{OFF}. Furthermore, the flexible devices demonstrated remarkable reliability, maintaining stable retention time and consistent performance across multiple cycles. These devices maintained decent switching upon bending up to a radius of 7 mm. This chapter highlight the enhanced performance of flexible RRAM devices achieved using PVP:MoS_2/TiO_2 bilayer as the switching layer, emphasizing their low operating voltage and improved functionality [Saini et al., 2023].

4 .1 Introduction

In the recent trend of digital and IoT world, there is always an increasing demand for reliable memory to store data. Emerging resistive RRAM is one of the excellent choices for non-volatile memory due to its fast-switching speed, simple structure, and low power consumption properties [Lanza et al., 2019, Wong et al., 2012]. The structure of RRAM is identical to a metal–insulator–metal capacitor, where resistive switching materials are used as a dielectric material between the metal electrodes. There are mainly three types of structures like common BE, crossbar, and 3D stack crossbar used to fabricate the RRAM devices. In common BE RRAM; the bottom contact is shared among all the top contacts present on the same sample. The crossbar array, the cross points of the perpendicularly fabricated word lines, and bit lines are used as memory cells to store the data [Deng et al., 2013]. The main issue in crossbar array is sneak path current and large power consumption. In 3D crossbar structure, layers can be stacked vertically or horizontally. A separate selector for each memory cell can be used to reduce the issue of sneak path current [Luo et al., 2016]. Among these RRAM structures, common BE structure is simplest and easy to fabricate. RRAM can store the data in the form of a LRS and HRS due to filament formation or rupture across the electrodes [Zahoor et al., 2020]. On the basis of filament formation between electrodes, RRAM device can be classified as a conducting bridge RRAM and metal oxide RRAM. In conducting bridge RRAM, top metal contact is made by electrochemically active material Ag or Cu and bottom contact should be chosen from any electrochemically inert material [Jana et al., 2015]. When positive bias is applied on the top contact of the device, Ag or Cu metal will be oxidized to Ag^+ or Cu^{z+} (where z can be 1 or 2) due to an electrochemical reaction [Valov et al., 2011]. The applied electric field forces the positive metal ions drift through the active switching layer. The oxidized metal ions will be reduced to the inert bottom contact. In this continuous process, conducting filament is formed across the electrodes which switch the device's resistive state. In metal oxide RRAM, oxygen vacancy plays a crucial role in forming the filament [Shringi et al., 2022, Wong et al., 2012].

To demonstrate high performance RRAM devices, various dielectric materials including inorganic materials such as titanium dioxide (TiO_x), aluminum oxide (AlO_x), hafnium oxide (HfO_x), and tantalum pentoxide (Ta_2O_5) [Trapatseli et al., 2016, Lodhi et al., 2022, Jin et al., 2021, Shen et al., 2019], organic polymers like polyvinylcarbazole (PVK), polyvinylpyrrolidone, polyvinyl alcohol (PVA) [Li et al., 2018, Rehman et al., 2016, Zhang et al., 2020], and 2D materials like GO, MoS_2, WS_2 and $MoSe_2$ [Varun et al., 2020, Varun et al., 2020, Jian et al., 2022, Lee et al., 2019, Saini et al., 2023], are investigated for resistive switching. RRAM devices have generated a lot of interest as a means of data storage for flexible electronics [Han et al., 2013], due to advantages of being thin, light weight, foldable, stretchable, and suitable for wearable electronics [Han et al., 2013, Singh et al., 2019]. A hybrid structure of polymer with inorganic material is integrated with rigid and flexible memory for high values of endurance, retention time, and

I_{ON}/I_{OFF}, along with low voltage operation and mechanical stability [Saini et al., 2023]. Metal oxide TiO_2 has a high reversible capacity with higher structural stability in RRAM devices [Pham et al., 2016]. TiO_2 has the most favorable. capabilities like data storage for long periods of time, and fast switching in comparison to other metal oxides like HfO_2, ZrO_2 etc,. and high k dielectric (k = 86–170) with wide band gap [Acharyya et al., 2014]. Moreover, MoS_2 is a widely explored TMD 2D material in RRAM devices to enhance the switching behavior [Wang et al., 2018]. The composition of MoS_2 with other polymers such as PVP and PVA has shown improvement in the RRAM device performance including improved switching window and low SET/RESET voltages [Rehman et al., 2016]. Though there are reports on the use of nanocomposite with polymers in RRAM devices to improve performance [26], this area is still underexplored. Here, a bilayer of high-k dielectric TiO_2 with composition of PVP: MoS_2 is explored for its switching behavior in both rigid and flexible RRAM devices with Ag/(PVP:MoS_2)/TiO_2/ITO structure.

4.2 Fabrication of Rigid and Flexible RRAMs

RRAM devices were fabricated on ITO coated glass and flexible PEN substrate. Figure 4.1(a) represents the schematic structure of the fabricated device. Substrates were firstly cleaned by bath ultrasonication method for around 15 min in isopropyl alcohol (IPA) and then rinsed in DI water followed by drying with nitrogen. A TiO_2 (10 nm thickness) layer was deposited over the ITO coated BE using the Savannah (S200) thermal atomic layer deposition (ALD) technique using Tetrakis(dimethylamido)titanium (IV) and H_2O as precursors at 150°C. Molybdenum(IV) sulfide (MoS_2) (Mw :160.07 g/mol) and PVP (Mw ~ 25000) were purchased from Sigma Aldrich. Liquid exfoliation process was used to prepare the MoS_2:PVP solution [Saini et al., 2022]. The composite solution of MoS_2:PVP was prepared by ultrasonication for up to 12 hour continuously and then it was kept carefully to settle down for 72 hour. The solution was deposited by spin coating at 4000 rpm for 45 seconds. To improve the film uniformity, both rigid and flexible samples were annealed on hot plate at 60 °C for 1 hour. The thickness of MoS_2:PVP was measured to be ~100 nm. At final fabrication step, top Ag contacts (~200 nm thickness) were thermally evaporated through shadow mask under the high vacuum of 1.2×10^{-6} torr. All the electrical characterizations were performed using Keithley 4200 SCS semiconductor parameter analyzer.

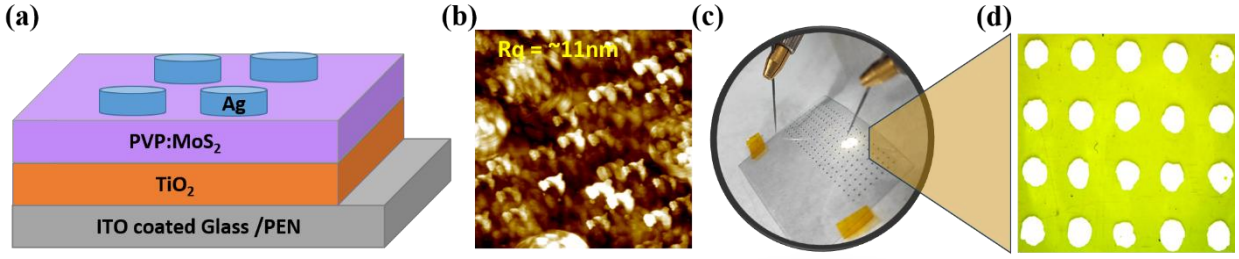


Figure 4.1 (a) Schematic structure of fabricated RRAM device, **(b)** AFM image of TiO_2/(PVP:MoS_2) film on rigid substrate, **(c & d)** digital picture of flexible sample.

4.3 Results and Discussion

Figure 4.1(b) shows the AFM image of TiO_2/(PVP:MoS_2) surface on glass substrate. The root mean square value of roughness was found to be ~11 nm, which indicates smooth surface of the film. The digital picture of the fabricated flexible RRAM is depicted in Figure 4.1(c & d). Resistive switching behavior of the rigid and flexible RRAM devices are shown in Figure 4.2(a) and (d) respectively. Initially, all the fabricated devices were in HRS and the filament formation process was required to SET the device or to shift from HRS to LRS. The continuous voltage sweep pulse was carefully applied from 0 → V_{max} → 0 → − V_{max} → 0 across BE and TE. Both rigid and flexible RRAM devices are switched from HRS to LRS at V_{SET} (~1 V and ~1.5 V) as shown in Figure 4.2(a) and (d) respectively. The filament rupture occurs when applied a negative sweep voltage result in an abrupt decrease of current and the devices reach HRS. V_{RESET} of ~−1.2 V and ~−0.7 V, are required for rigid and flexible RRAM devices respectively resulted in abrupt decrease of current and the device reaching HRS. As it can be seen from these results, an excellent

memory window of more than 10^3 with distinct SET and RESET voltages was achieved. Figure 4.2 (b & e) shows the retention characteristics and repeatability of the rigid and flexible devices.

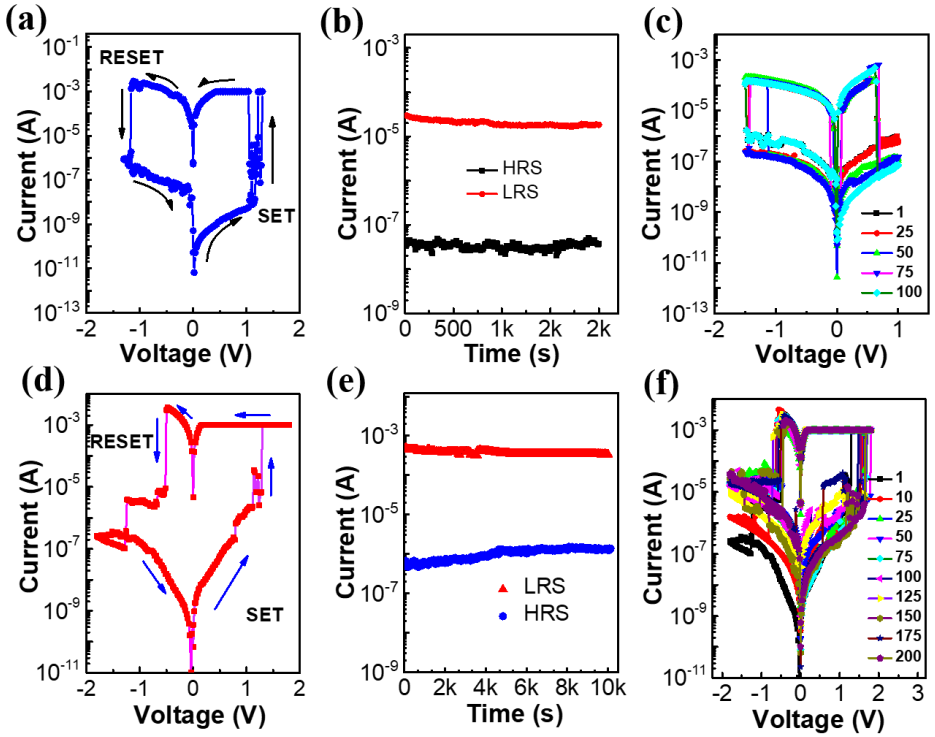


Figure 4.2 *I-V* characteristics of Ag/(PVP:MoS_2)/TiO_2/ITO **(a)** rigid and (d) flexible substrate respectively. Retention time characteristics for rigid **(b),** and flexible (e) RRAM device. Multiple cycle repeatability for rigid **(c)** device up to 100 cycles, and **(f)** flexible device of *I–V* up to 200 cycles.

The retention plot for rigid device is shown in Figure 4.2(b). For the same, a fixed bias of minimum read voltage i.e. 0.2 V was applied across the electrodes for both HRS and LRS. No major degradation was observed for 2000 s and a decent I_{ON}/I_{OFF} of around 10^3 was maintained. The same process was later followed on flexible device, and up to 10000 s of retention was measured as shown in Figure 4.2(e). The repeatability of resistive switching up to 100 cycles without any remarkable degradation in the switching window of rigid RRAM device is shown in Figure 4.2(c). Similarly, multiple cycle repeatability of flexible device for 200 cycles is plotted in Figure 4.2(f). It can be observed that the cycle-to-cycle variation in flexible device is slightly higher than in rigid device. In both the fabricated devices, first cycle does not require higher voltage for filament formation than subsequent cycles. Thus, we can say it is a forming free device due to sufficient compliance current applied and presence of TiO_2 layer [Yang et al., 2020]. Both rigid and flexible devices exhibited similar device-to-device variability, as indicated through the comparison of V_{SET}, V_{RESET}, and I_{ON}/I_{OFF} given in Table 4.1 which summarizes the average performance parameters of five randomly chosen Ag/PVP:MoS_2/TiO_2/ITO RRAM devices on both rigid and flexible substrates. Though a shift in both V_{SET} and V_{RESET} in positive direction (0.33 and 0.48 V) can be seen from rigid to flexible devices possibly due to difference in substrate surface properties, both types of devices showed almost identical device-to-device variation in V_{SET} and V_{RESET} with standard deviations of ~10% and ~25% respectively. Moreover, flexible devices exhibited higher I_{ON}/I_{OFF} (~10^6) compared to rigid devices (~10^4) indicating enhanced memory window.

Table 4.1: Comparison of Switching Parameters of Ag/PVP:MoS_2/TiO_2/ITO RRAM Devices on Rigid and Flexible Substrates

Ag/PVP:MoS_2/TiO_2/ITO	V_{SET} (V)	V_{RESET} (V)	I_{ON}/I_{OFF}
Rigid	1.11 ± 0.12	-1.18 ± 0.30	~10^4

Flexible	1.44 ± 0.15	-0.70 ± 0.17	~10^6

To explore the effect of compliance current in rigid and flexible devices, the same was varied from 100 µA to 1 mA, and effect of the same was studied on current in the SET side. For electrical study of RRAM device, compliance current plays a very crucial role. The primary role of it is to lit the maximum current flowing in the devices which prevent the device from any permanent damage. Moreover, a suitable sufficient value of the same is needed to achieve the SET state operation. On the other hand, having higher compliance leads to high power dissipation from the devices during switching operations. Figure 4.3(a) and (b) show the *I–V* characteristics of rigid and flexible RRAM device respectively under compliance current variation. Some of the important device characteristics like multi-level operation depend on the various level of compliance current [Russo et al., 2009], where every single state defines different bit storage in multibit operation on a single RRAM device [Kozicki et al., 2005].

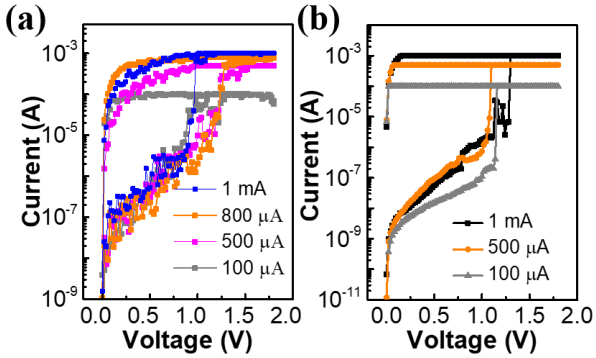


Figure 4.3 ***I–V*** characteristics with varying compliance current for rigid **(a),** flexible substrate **(b)** RRAM device.

By controlling the compliance current, the physical dimensions of conducting filament can be tuned. Thus, device operation at different compliance currents is an important characteristic of RRAM. Our results indicate that these devices offer possibility for compliance current reduction, which will eventually lead to low power dissipation.

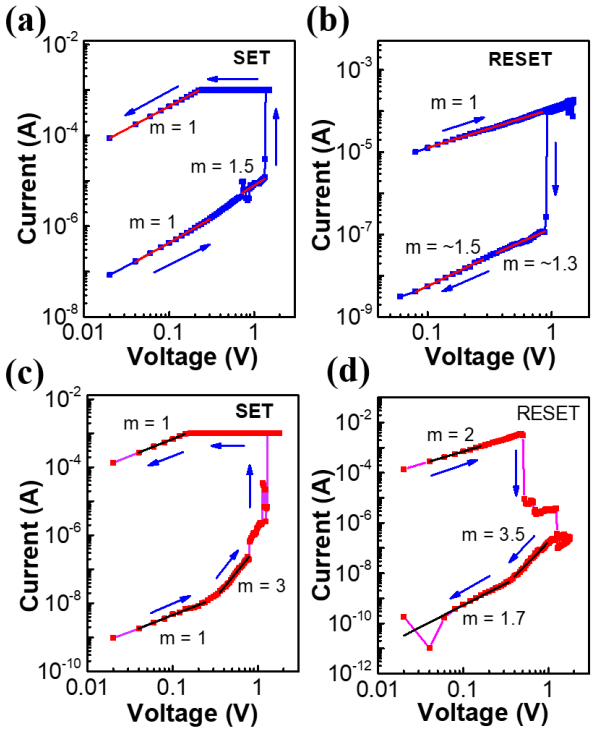


Figure 4.4 Conduction mechanism in SET and RESET are shown for rigid in **(a) & (b),** and flexible in **(c) & (d)** respectively, demonstrated through double log *I–V* plots.

To understand the conduction mechanism of both fabricated de vices, linear fitting of the double log (I–V) curve in the positive cycle (SET) and negative cycle (RESET) is performed as illustrated in Figure 4.4. Conduction mechanism of rigid device for SET and RESET is plotted in Figure 4.4(a) and (b). In RRAM devices, switching is possible due to various types of conduction mechanisms like ohmic, space charge limited current (SCLC), hopping, tunneling or Poole–Frenkel conduction. In linear fitting curve, for low value of voltage a slope value of m =~1 indicates the ohmic region of the device. The ohmic conduction occurs due to the trap sites inside the dielectric are not filled completely and also due to thermally generated charge carriers. The electric field increases, when the voltage across the electrodes increases, as shown in Figure 4.4(a). The slope of the log (V) versus log (I) graph reaches a maximum of m = 1.5. Inside the dielectric layer, all trap sites are entirely filled, and a sharp spike in current indicates that the device has reached the LRS or SET state. The sharp switching in current follows the space charge limited conduction (SCLC), which is governed by the Child's law [Wright, 1961]:

$$JSLC = q \in m\mu\theta V^2/8d^3 \tag{4.1}$$

where ε_m indicates the dielectric constant of the material, θ is the ratio between free and total carrier density, μ identifies the mobility of charge carriers, V is the applied voltage, and d is the spacing between two electrodes. Since, the filament is already present, initially ohmic conduction was observed which is clearly seen by the slope value m = 1. After reaching the RESET voltage sudden decrease in current is observed which indicates the device has entered HRS or RESET state. After breakage of the filament, current voltage (I–V) characteristic follows the Child's Law (which is indicated by the slope value m = 1.5 and 1.3) as shown in Figure 4.4(b).

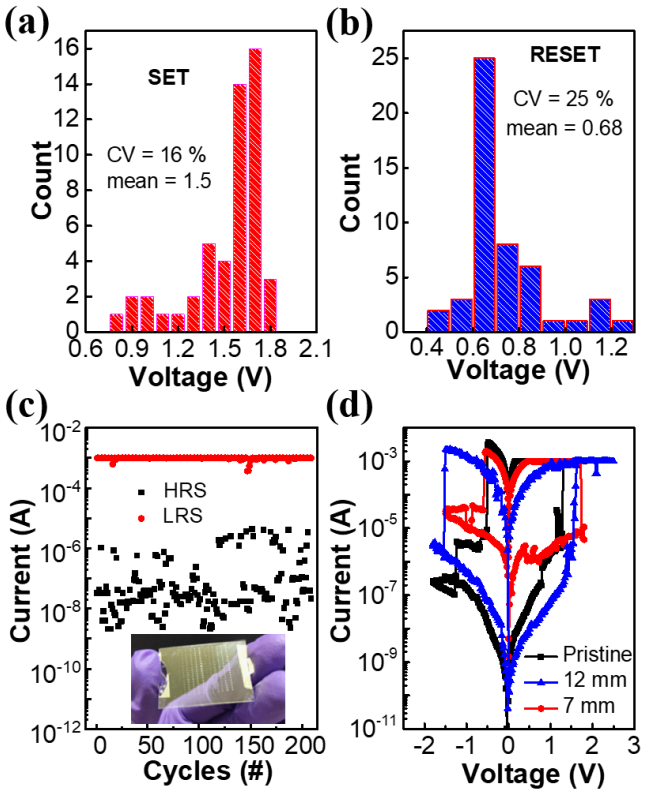


Figure 4.5 Cycle to cycle variation of operating voltage distribution for SET **(a)**, and RESET **(b)**. **(c)** Endurance of consecutive 200 DC cycles at read voltage of 0.2 V. Digital image of flexible device is shown in the inset. **(d)** ***I–V*** characteristics at different bending radius up to 7 mm.

Similarly, conduction mechanism was studied by the linear fitting of double log (I–V) plots of flexible device for SET and RESET as shown in Figure 4.4(c) and (d). Here, fitted slope value m = 1 indicates ohmic region and the slope value from 1 < m = 2 indicates the SCLC mechanism. Slope values of 3 and 3.5 are also present in the linear fitted graph, indicating the trap filled limited

conduction mechanism. To investigate the reliability of flexible RRAM devices, cycle to cycle variation, endurance, and device bending stability up to 7 mm was studied.The variation of SET and RESET voltage of consecutive 50 cycles using CV are depicted in Figure 5(a) and (b) respectively. The CV can be calculated by using the following formula [Lee et al., 2022].

$$CV = \left(\frac{\sigma}{|mean|}\right) \times 100\% \quad (4.2)$$

σ indicates the standard deviation. The CV of cycle-to-cycle variation of first 50 consecutive DC cycles is 16% for SET and 25% for RESET voltage. It indicates that V_{SET} has 16% probability to be 1.5 V as depicted in Figure 4.5(a) and V_{RESET} has 25% probability to be −0.68V as shown in Figure 4.5(b). Figure 4.5(c) shows the endurance characteristics of more than 200 consecutive DC cycles of flexible RRAM device. A digital image of a flexible substrate with multiple devices is shown in the inset of Figure 4.5(c). Both LRS and HRS are taken at read voltage of 0.2V. It can be seen in the results that LRS is stable for all DC cycles whereas acceptable variation in HRS was observed, probably due to random rupture of filament. Finally, the effect of bending on the electrical the flexible RRAM devices was investigated. For the same, devices were bent a radius of 12 mm and 7 mm respectively for a duration of 15 minutes for each case. The variation I–V characteristics upon bending are shown in Figure 4.5(d). As it can be, the I_{ON}/I_{OFF} of the device decreases upon bending. The I_{ON}/I_{OFF} was found to be ~10^5 in the pristine state, ~10^4 at a 12 mm bending radius, and ~10^3 at 7 mm, indicating a gradual yet consistent switching behavior under bending. These results indicate that the hybrid bilayer combination of (PVP:MoS_2) with TiO_2 can be a promising choice for switching layers in flexible RRAM devices. The results confirm the excellent switching behavior of duly engineered layer facilitating conductive bridge resistive switching by Ag electrodes. This switching behavior depends on energy levels of various materials and electrodes.

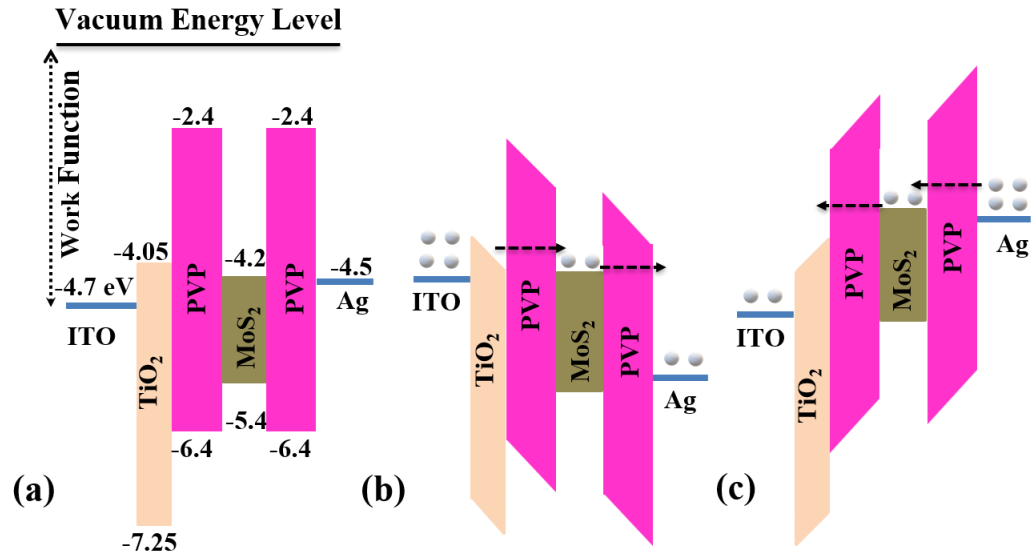


Figure 4.6 Schematic energy band diagram for Ag/(PVP:MoS_2)/TiO_2/ITO RRAM device. **(a)** Before biasing, **(b)** during SET state, and **(c)** during RESET state.

The energy band diagram of proposed Ag/(PVP:MoS_2)/TiO_2/ITO RRAM device is depicted in Figure 4.6. The work function of ITO (BE) and Ag (TE) are −4.7 eV and −4.5 eV respectively. The highest occupied molecule orbital (HOMO) and lowest unoccupied molecular orbital (LUMO) of PVP are −6.4 eV and −2.4 eV respectively as shown in Figure 4.6(a). The energy levels and work function differences provide first hand idea of the required voltage levels. The corresponding bending in energy bands will occur upon application of voltages. When a positive bias is applied on the Ag electrode, charge carriers flow in this state clearly represents the injection and trapping of electron as shown in Figure 4.6(b). Upon further increase in voltage bias beyond V_{SET}, the amount of charge carriers tunneling through the PVP will be increased resulting in sharp

increase in current. Similar conclusion can be derived for the RESET mechanism using the band diagram as shown in Figure 4.6(c). Figure 4.7 shows the schematic of switching mechanism of filament formation and rupture in SET and RESET states. When positive voltage is applied across the TE and BE, Ag electrode oxidizes to Ag^+ ions and due to the electric field, these ions start migrating towards the BE. In the same manner, the electrons start moving towards TE from BE and Ag^+ will become Ag. The accumulation of electro chemically Ag atoms helps to form the conducting filament. Upon complete conducting filament formation, a sharp change in current will be observed at the V_{SET} and device will shift from HRS to LRS as depicted in Figure 4.7(a). The data will be stored in the memory until the negative supply V_{RESET} is applied across the TE and BE. This behavior indicates the non-volatile property of RRAM.

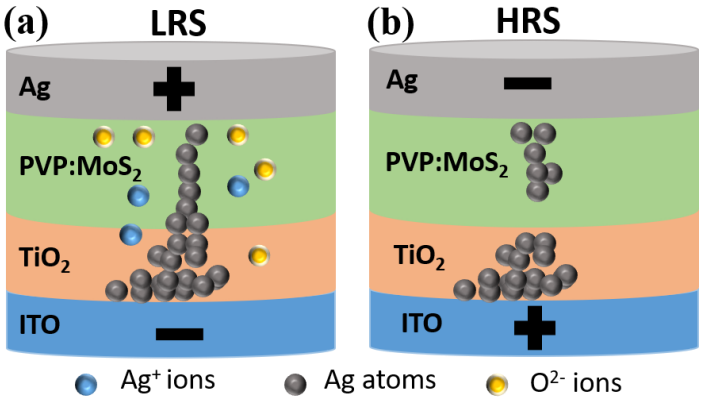


Figure 4. 7 Switching mechanism for SET **(a)** and RESET **(b).**

Upon application of negative voltage to TE, a high current running starts flowing in opposite direction through conductive filament. This results towards a Joule heating-assisted break down causing Ag^+ ions to move towards the TE. These ions will then reduce to Ag, as depicted in Figure 4.7(b).

Table 4. 2 : Summary of performance parameters of some recently reported RRAM devices with PVP as an active material component on rigid and flexible substrates.

Device Structure	Substrate/ Type	V_{SET} (V)	V_{RESET} (V)	I_{ON}/I_{OFF}	*Endur.*	Ret.	Ref.
Al/PVP-PBD/ITO	Glass/Rigid	-1.4	3.55	10^4	300	1×10^4	[Sun et al., 2015]
Al/PVP-DDQ/ITO	Glass/Rigid	3	-1.3	10^6	20	1×10^4	[Vyas et al., 2016]
Pt/N-doped MoS2-PVP/ITO	Glass/Rigid	0.75	-0.5	NA	200	3×10^3	[Wu et al., 2017]
Ag/PVP/HfO_x/ITO	Glass/Rigid	1.03	-0.68	80	2000	7×10^3	[Varun et al., 2018]
Ag/PVP:GO/TiO_x/ITO	Glass/Rigid	1	-2	10^3	128	7×10^3	[Lodhi et al., 2022]
Al/PVP-GQD/HfOx/ITO	PET/Flexible	1.53	-0.76	68	100	7×10^3	[Kim and Hwang, 2021]
Ag/PVP:GO/HfO_x/ITO	PET/Flexible	0.6	-1.46	10^3	150	1×10^4	[Varun et al., 2020]
Ag/PVP:MoS_2/HfO_x/ITO	PET/Flexible	~1	NA	10^4	100	NA	[Varun et al., 2020]
Ag/PVP:MoS2/TiO_2/ITO	Glass/Rigid	~1	-1.1	10^4	100	2×10^3	[Saini et al., 2023]
Ag/PVP:MoS_2/TiO2/ITO	PEN/Flexible	1.5	-0.68	10^3	200	1×10^4	[Saini et al., 2023]

Table 4.2, compares the performances of few recently reported RRAM devices based on PVP as an active material on rigid and flexible substrates with fabricated devices. As it can be seen, Ag/(PVP:MoS_2)/TiO_2/ITO RRAM devices compare very well in terms of performance compared to other similar reports. More importantly the SET and RESET voltages for the devices reported in this work are in the lower side compared to other reports with similar current I_{ON}/I_{OFF}, retention, and endurance characteristics like [Sun et al., 2015, Varun et al., 2020]. The reported retention time for all these cases is in the range of 10^3–10^4. The device had shown the capability of being evaluated for higher retention time.

4.4 Conclusion

RRAM devices with Ag/(PVP:MoS_2)/TiO_2/ITO hybrid structure on both rigid and flexible substrate have shown reliable resistive switching with low values of V_{SET} and V_{RESET} for rigid (1.0 V, -1.2 V) and flexible (1.5 V, -0.7 V) devices. Non volatile memory behavior with excellent retention up to 10000 seconds and decent I_{ON}/I_{OFF} more than 10^3 was achieved. The endurance of more than 200 DC cycles indicates the good repeatability of the device. Log (V) versus log (I) graph showed dominating ohmic conduction and SCLC mechanism in the devices. Bending stability up to 7 mm indicate that these bilayers with 2D material and polymers can be excellent alternatives for switching layer in RRAM devices for polymer and flexible electronics.

…